Microscopy AND
Microanalysis

© MICROSCOPY SOCIETY OF AMERICA 2013

Development, Preimaginal Phases and Adult Sensillar Equipment in *Aganaspis* Parasitoids (Hymenoptera: Figitidae) of Fruit Flies

José Tormos,[1,*] Luis de Pedro,[1] Francisco Beitia,[2] Beatriz Sabater,[2] Josep Daniel Asís,[1]
and Carlo Polidori[3]

[1]*Unidad de Zoología, Facultad de Biología, Universidad de Salamanca, 37071, Salamanca, Spain*
[2]*Instituto Valenciano de Investigaciones Agrarias, Unidad Asociada de Entomología IVIA/CIB-CSIC, Apartado Oficial. 46113-Montcada, Valencia, Spain*
[3]*Departamento de Biodiversidad y Biología Evolutiva, Museo Nacional de Ciencias Naturales (CSIC), C/ José Gutiérrez Abascal 2, 28006 Madrid, Spain*

Abstract: *Aganaspis daci* and *Aganaspis pelleranoi* (Hymenoptera: Figitidae) are important parasitoids of fruit flies. Here we studied, with light and scanning electron microscopy, aspects of their morphology that could help with plans to mass rear and thus contribute to improved pest control (preimaginal phases) and to shed light on parasitoid-pest relationships (sensillar equipment). The two species present a stalked egg, eucoiliform first and second-instar larvae and hymenopteriform third instar and mature larvae. The first instar presents tegumental differentiations in the mesoma and first metasomal segment in *A. daci*, but not in *A. pelleranoi*, while unlike other figitids, neither species displays setae in the mesosomal processes. Second and third instar and mature larvae present tegumental differentiations in *A. daci*, but not in *A. pelleranoi*. The moniliform (female) and filiform (male) antennae of *A. daci* and *A. pelleranoi* harbor seven types of sensilla, four of them (sensilla campaniformia, sensilla coeloconica type II, and two types of sensilla trichoidea) described here for the first time in Cynipoidea. The largest sensilla were the multiporous placoid sensilla, which were smaller and more numerous in *A. pelleranoi*. Species also differed to some extent in morphology of sensilla coeloconica. Observations on the ovipositor revealed the presence of coeloconic sensilla on Valva I in both species.

1. Introduction

The genus *Aganaspis* Lin (Hymenoptera, Figitidae, Eucoilinae) comprises six species of parasitoids of tephritid flies (Díaz et al., 2006). Within Eucoilinae, the genus is unique in that it is the only one which has been successfully used in biological control of fruit flies (Clausen, 1978; Wharton et al., 1981; Baranowski et al., 1993). In particular, efficient fruit fly pest control has been recorded for *Aganaspis daci* (Weld) and *Aganaspis pelleranoi* (Brèthes), two larvo−pupal solitary primary endoparasitoids. *A. daci* was first recorded in 1951 as a larval parasitoid of *Dacus* spp. in Malaysia and Taiwan (Weld, 1951). In the Mediterranean basin, it was first recorded in 2003, on the Greek island of Chios, and restricted to medflies [*Ceratitis capitata* (Wiedemann)] as a host in fig fruits (Papadopoulos & Katsoyannos, 2003). Lately, it has spread to Israel and Egypt, from a USDA-ARS Hawaii colony (El-Heneidy & Ramadan, 2010). *A. pelleranoi* is a neotropical larval−pupal parasitoid, which attacks a wide variety of tephritid hosts, with distribution from México to Argentina (Ovruski et al., 2000) and was also recently reported in Spain.

In 2003, a biological control project was started with several imported exotic egg−larval parasitoids, *Fopius arisanus* (Sonan), *Diachasmimorpha tryoni* (Cameron) and *Diachasmimorpha longicaudata* (Ashmead), and following the release trials, several specimens of *A. daci* were recovered from medfly larvae collected from figs in the summer of 2009−2010, opening the way for a new program with a native larval parasitoid. At present, biological studies of this parasitoid are being performed to assess its adaptability to mass rearing. Previously, in Spain, only the species *Spalangia cameroni* (Perkins) and *Pachycrepoideus vindemmiae* (Rondani) (Hymenoptera: Pteromalidae) were identified as native pupal parasitoids of medflies, with no records of *A. daci* in a four-year survey (2000−04; Beitia et al., 2009).

For both *A. daci* and *A. pelleranoi* there is some information about certain aspects of their biology (Ovruski, 1994; Ovruski & Aluja, 2002; Guimaraes & Zucchi, 2004); however, little is known of certain aspects of their morphology that could contribute to planning mass-rearing and thus pest control [preimaginal phases, having only been studied in *A. pellerenoi* by Ovruski (1994) and briefly in *A. daci* by Clausen et al. (1965)] and to better understand parasitoid−pest relationships (sensillar equipment). In addition, little attention has been paid to its developmental biology (Papadopoulos & Katsoyannos, 2003; Andleeb et al., 2010) and functional morphology (but see Clausen et al., 1965). Developmental biology studies, including morphological characterization of the preimaginal stages, may be important in identification of an insect at the species level before adult emergence and can simplify quantification of the impact of natural enemies in biological control programs (Bellows & Van Driesche, 1999; Llácer et al., 2005; Onagbola & Fadamiro, 2007; Tormos et al., 2009*a*, 2009*b*). Morphological

studies of antennal and ovipositor sensilla (OS) can help to corroborate the role of antennal sensilla and OS in locating, evaluating and accepting the host (Jervis et al., 2005; Baaren et al., 2007).

Most knowledge about preimaginal morphology in Cynipoidea wasps is due to the contributions of Vårdal et al. (2003) and Nieves-Aldrey et al. (2004), as well as other studies by Clausen (1972) and Evans (1987). Scarce information exists for the genus *Aganaspis* (see above). On the other hand, although antennal and OS have been studied in some Figitidae taxa (Butterfield & Anderson, 1994; Lenteren et al., 2007), they have not been described in the genus *Aganaspis*.

2. Materials and methods

2.1. Insects

The stages of preimaginal phases, morphology of antennae and ovipositor, and data on the developmental biology of *A. daci* were obtained from rearing this parasitoid at the installations of Instituto Valenciano de Investigaciones Agrarias (IVIA Valencia, Spain), in a climate chamber (Sanyo MLR350) at 25 ± 0.2 ºC , $65 \pm 10\%$ RH, and a 16L:8D photoperiod. For rearing, third-instar larvae of the Mediterranean fruit fly were used as hosts, and parasitoids, confined in a plastic cage (35 x 30 x 36 cm) with ventilation, were fed with honey impregnated on strips of blotting paper, sugar, and water.

The morphology of antennae and ovipositors of *A. pelleranoi* were analyzed in eight specimens obtained from a collection from México. Preimaginal phases of this species were not studied here because a detailed description is already given in Ovruski (1994). This description is used for comparison with our results for *A. daci*.

To study development and morphology of the immature stages, 2000 third-instar larvae of *C. capitata,* which had been exposed to *A. daci* for 4 h, were taken from a plastic rearing cage where large numbers of *A. daci* females and males had cohabited for a number of generations. Fifty larvae per plate were placed in 40 Petri dishes (9 x 1.5 cm). One hundred parasitized larvae and pupae per day were periodically dissected in Insect Ringer's solution on depression slides in order to examine development and morphology of the different phases. Additionally, in order to determine the time each of the sexes took to develop, 1000 third-instar larvae previously exposed to parasitoids were allowed to develop in order to obtain *A. daci* males and females.

One hundred and twenty-five eggs, 220 immature larvae, 36 mature larvae, and 78 pupae of *A. daci* were fixed and preserved in 70% EtOH for subsequent study and description.

Descriptions are based on several specimens. The length of the egg and first-instar larval body was measured from the posterior tip to the transition between body and peduncle. The length of the first- and second-instar larva body was measured from the anterior tip to the transition between the body and the peduncle. The length of the mandibles is the maximum length: measured from the points of articulation with the head to the pointed tip. The ensuing descriptions essentially employ the terminology and organization used by Tormos et al. (2009*a*, 2009*b*). Data are presented as range and mean values ± standard deviation (SD). Student's *t*-tests to determine inter-sexual differences were performed using the SPSS statistical software package (v15.0).

Immature phases studied are deposited at the IVIA. Adults are deposited at the Museo Nacional de Ciencias Naturales (Madrid, Spain).

2.2. Histological methods, stereomicroscopy and Scanning Electron Microscopy (SEM)

2.2.1. Preimaginal stages

For light microscopy preparation of eggs and larval stages, the methods described by Tormos et al. (2003, 2004, 2007, 2009*a*, 2009*b*) were employed, with the exception of first-instar larvae for which the method used by Roskam (1982) to prepare Eurytomidae larvae was followed. In this case the larvae were macerated in warm 80% lactic acid and then washed in 30% ethanol, with fatty substances removed in acetone before dehydration and preparation. Photos and measurements to the nearest 0.01 mm of different structures of the preimaginal phases were taken under a Leica MI65C microscope, equipped with a Leica EC3 camera using the Application Suite Version 3.6.O (Imaging Software Integrates, Leica Microsystems Imaging Solutions) (IVIA).

Sketches were made with a drawing tube and subsequently using the Adobe Illustrator CS5 application to create and manipulate the vector drawing. For SEM, live samples were frozen in slush N_2 and attached to the specimen holder of a CT-1000C Cryo-transfer system (Oxford Instruments, Oxford, UK) interfaced with a JEOL JSM-5410 SEM (Universidad Politécnica de Valencia, Valencia, Spain). Samples were then transferred from the cryostage to the microscope sample stage, where the condensed surface water was sublimed by controlled warming to −90º C. Then, samples were transferred again to the cryostage and sputter-coated with gold. Finally, the samples were returned to the microscope sample stages for visualization at an accelerating voltage of 15 keV.

2.2.2. Sensilla of antennae and ovipositors

The antennae of three females and three males of both species were analyzed while the ovipositor was studied in two females of both species. The sensilla on antennae and ovipositors were studied by analyzing SEM images obtained using an ESEM QUANTA 200 microscope (FEI Company, Oregon, USA) at the Museo Nacional de Ciencias Naturales (Madrid, Spain). High vacuum conditions [resolution: 3.0 nm at 30 kV (SE), 10 nm at 3 kV (SE), and 4.0 nm at 30 kV (BSE)] were used on gold-coated samples. The accelerating voltage was 26 kV, the high vacuum was 0.40–0.50 torr, and the working distance was 10 mm. Antennae and ovipositors were observed in dorsal, ventral and lateral view.

For the sensilla inventory, we primarily followed the classification of sensilla by Callahan (1975), Isidoro et al. (1996), Keil (1999) and Romani et al. (2010a), based on morphological characters. This classification should be considered, for some sensilla types, as preliminary because the internal structure and function of different types of sensilla are not yet fully known (Altner, 1977). The flagellomeres were designated F1 to F11 for females and F1 to F13 for males, in a proximal to distal direction.

The antennae were observed in dorsal, ventral and lateral views. The number of sensilla was not recorded exactly on each segment due to orientations of some twisted antenna. However, we counted them in certain well-visible segments. The sample of sensilla used for size calculations came from two or three antennae from each species, depending on their visibility/definition in the SEM images. Because of the small sample size (number of individuals and antennae), we give numerical results as ranges rather than means.

In both cases, for the preimaginal phases as well as for the morphological analysis of antennae and ovipositors, we calculated lengths and widths of structures and body parts from pictures taken at higher magnifications (up to 300×), importing them into ImageJ software (National Institutes of Health, Bethesda, MD, USA), where calculations were made.

3. Results

3.1. Development of *A. daci*

The *A. daci* life cycle can be divided into four phases: egg (embryonic), larval, pupal, and adult (Table 1). At 25 °C, the life cycle takes ~ 32–33 days to complete. Development time (32.08 ± 2.54 days in females and 28.23 ± 2.52 days in males) differed significantly between the two sexes (Student's *t*-test, *F*-test for equal variance: $F = 0.986, \leq 0.100$; df = 624, $t = 7.784$, $p < 0.001$), being greater for the female. The mating period started after adult emergence. The embryonic phase of *A. daci* (0–82 h) begins with the injection of an egg into a third-instar host

larva. The embryo hatches into the first-instar endoparasitic eucoiliform larva (80–120 h). The first-instar molts into a still "endoparasitoid" hymenopteriform second instar (around ~ 108 h). The second-instar molts into a third-instar larva, which emerges from the host body cavity, marking the endo to ectoparasitic transition. This larva occupies both internal and external positions in the host pupa and develops two respiratory mechanisms, like *A. pelleranoi* (Ovruski, 1994), one cuticular, and another tracheal. During this "ectoparasitic phase" (~ 100 h), this instar larva feeds externally within the host puparium. The third-instar larva molts into a fourth-instar larva (mature larva) whose feeding continues externally on what remains of the host pupa and is very sluggish, occupying the greater part of the puparium host (~ 140 h). After feeding is completed, host remains (meconium) are excreted, and the fourth-instar larva decreases in size and becomes a prepupa (postdefecating mature larva). The prepupa gives rise to the pupa (~ 220 h), which is characterized by a halt in growth and rapid differentiation. The adult phase begins with the emergence of free-living adult male (~ 672 h) and female (~ 770 h) wasps.

3.2. Preimaginal stages of *A. daci*

3.2.1. Egg

The embryonic phase of the life cycle of *A. daci* begins with the injection of one or more eggs into the hemocoel of the last instar of a *C. capitata* larva. Approximately similar in size to the *A. pelleranoi* egg (Ovruski 1994; Table 1), the *A. daci* egg also presents a stalk on the anterior end and, like the *A. pelleranoi* egg, is surrounded by a thin, translucent, and smooth chorion (Fig. 1A), the embryo, vitelline membrane and chorion becoming discernible at 24 h after ovoposition (Fig. 1B). At 48 h after oviposition, the stalk has practically disappeared (Fig. 1C) and after 72 h the embryo shows signs of body segmentation (Fig. 1D). SEM observation of this last stage (Fig. 1E) shows that the chorion surface lacks apparent sculpturing, but a specialized area with a softer chorion can be seen at the anterior end of the egg (Fig. 1F). In all cases ($n = 25$) the eggs hatched at between 80 and 82 h after oviposition at 25 ± 0.2 ºC, $65 \pm 10\%$ RH, and a 16L:8D photoperiod.

Table 1. Measurements taken on the different phases of development of *Aganaspis daci*.*

Phase	Variable	Measurement (mm)**
Egg	Length	0.51 ± 0.004 [0.48–0.66] ($n = 125$)
	Maximum width	0.29 ± 0.03 [0.28–0.32] ($n = 125$)
Larva, first instar	Body length	0.91 ± 0.05 [0.87–1.17] ($n = 80$)
	Body width at the level of the metathoracic segment	0.21 ± 0.04 [0.18–0.23] ($n = 82$)
Larva, second instar	Body length	1.06 ± 0.03 [1.09–1.12] ($n = 14$)
	Body width at the level of the metathoracic segment	0.25 ± 0.03 [0.22– 0.27] ($n = 15$)
Larva, third instar	Body length	2.65 ± 0.03 [2.50–2.79] ($n = 26$)
	Body width at the level of the metathoracic segment	0.68 ± 0.05 [0.62– 0.74] ($n = 31$)
Larva, fourth instar	Body length	2.81 ± 0.02 [2.95–3.04] ($n = 12$)
	Body width at the level of the metathoracic segment	1.16 ± 0.03 [1.04–1.22] ($n = 25$)
	Cranium maximum width	0.57 ± 0.06 [0.53–0.57] ($n = 26$)
	Mandible length	40.63 ± 0.48 [31.25–51.22] ($n = 12$)
	Prepupa length	2.11 ± 0.09 [2.01– 2.13] ($n = 7$)
	Prepupa width	0.95 ± 0.10 [0.93– 0.99] ($n = 7$)
	Pupa length	1.82 ± 0.31 [1.6–2.00] ($n = 57$)

*Mean values ± SD, minimum-maximum range (in square brackets) and sample size (in brackets) are reported. All measures are in mm.
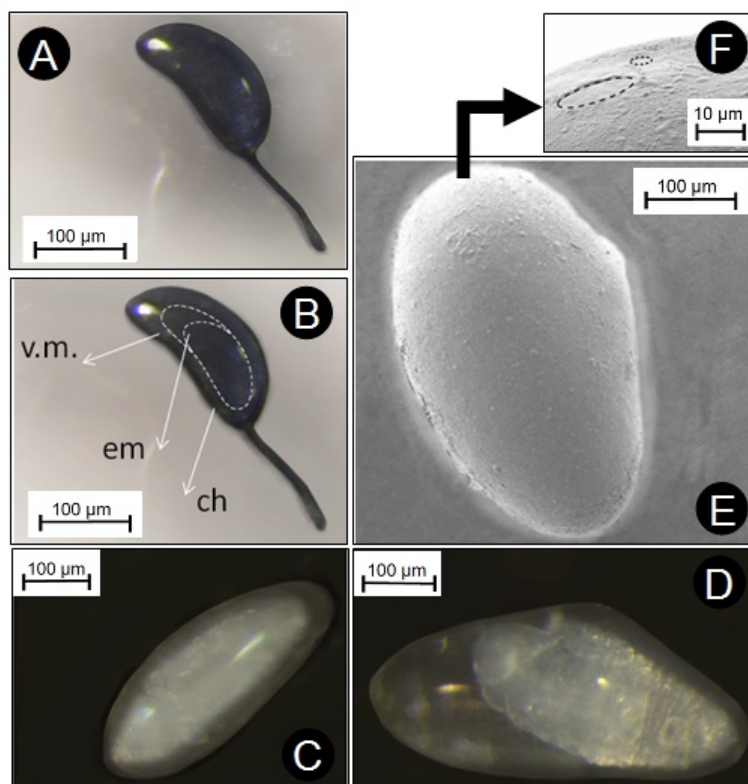
**Except in the mandibles that are in μm.

Figure 1. *Aganaspis daci* (Weld). Egg: (**A, B**) eggs at 24 h after oviposition; (**C, D**) eggs between 48 h (**C**) and 72 h (**D**) after oviposition [the dotted lines show the vitelline membrane (v.m.) and outline the embryo (em); an arrow shows the chorion (ch)]; (**E, F**): SEM pictures show eggs to have a smooth surface (**E**) and specialized anterior area with the chorion distinctly softer (**F**, see circles with dotted line).

3.2.2. Larva, First instar

First-instar larvae were eucoiliform (thoracic segments bear a pair of long ventral processes; posterior abdominal segments taper into a fleshy caudal region) type. This stage was observed between 80 h and the 5th day after oviposition when the host was in early pupa stage. General aspects and measurements are shown in Figures 2A, 2B, 2F and Table 1. Color is whitish and more or less translucent. Shape is subcylindrical with a defined and elongate head and 11 body segments. The cranium (Figs. 2A, 2B) is elongated with a prominent more or less tubular anterioventral "proboscis" (Figs. 2C, 2D) that has a large number of concavities – presumably sensory structures– and on whose apex the mouth is located, surrounded by several oral papillae. Inside the mouth there are the falcate mandibles (unidentate and more or less subtriangular). The gut is easily discernible. The head has at least 14 pairs of sensory structures. A pair of appendages (Figs. 2A, 2B, 2E), each measuring approximately half the body length (without tail), is present on each one of the three thoracic segments. A long spiny tail, measuring approximately two-thirds of the body length, and a short ventral process (Figs. 2F, 2G, 2H) emerges from the caudal segment. The lateral and ventral margin of the seventh

abdominal segment and basal end of the caudal segment have scale-like ornamentation (Fig. 2H). The integument of the mesosoma and first abdominal segment have numerous differentiations (Fig. 2E). The anus (Fig. 2G, see arrow) opens dorsally in the last abdominal segment. At the end of this period, the larvae lose all thoracic appendages and ventral processes.
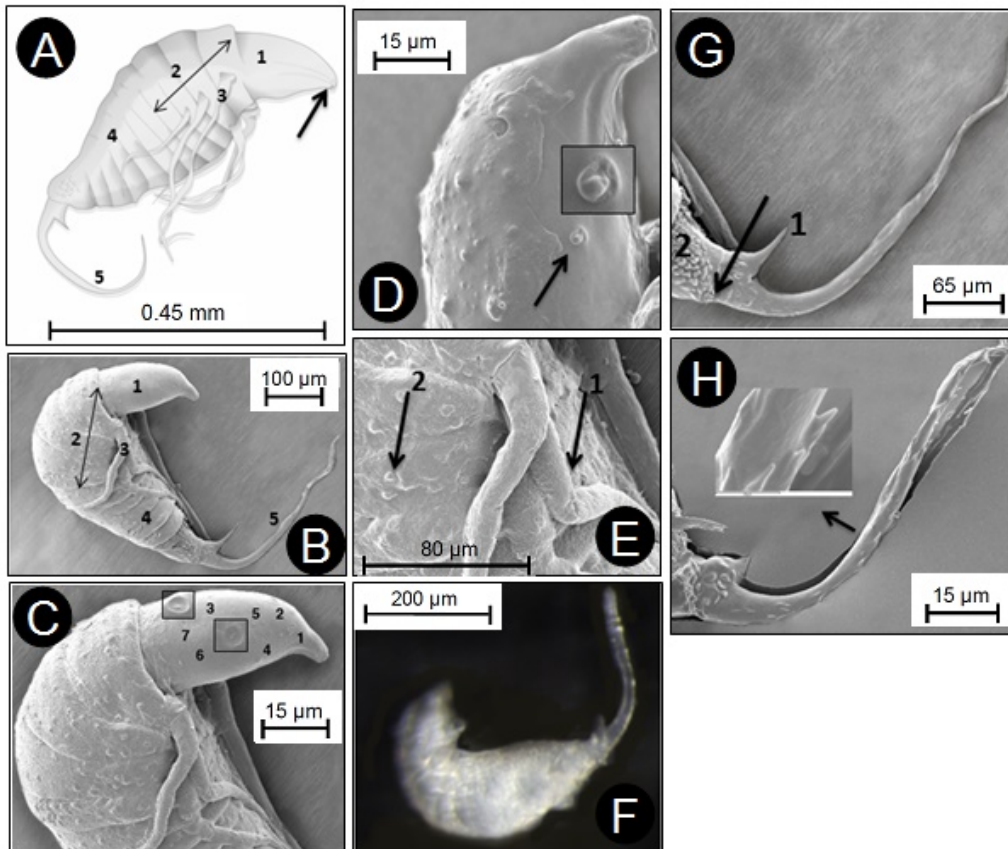

Figure 2. *Aganaspis daci* (Weld). Larval phase. First instar: (**A, B**) (under SEM): body showing the head (1), mesosoma (2) with long slender ventral thoracic processes (3), metasoma (4) and the caudal tail (5) [in (**A**), an arrow points to the mandibles]; (**C**) detail of the head showing presumed sensory structures of different types (numbers 1–7, see detail 3, 5 x 2.5); (**D**) detail of the head showing the "proboscis" and several tegumental differentiations of likely sensory value (an arrow points to a probable sensory structure, detail x 2.5); (**E**) detail of thoracic processes (see arrow 1) and tegumental differentiations (see arrow 2) present in mesosoma and first abdominal segment; (**F–H**) details of caudal segment showing tail with spines [(**H**) (under SEM), see arrow, detail x 2.5], ventral process [(**G**)–(1)], scale-like ornamentation on caudal segment [(**G**)–(2)], and anus position [(**G**) (under SEM), see arrow].

3.2.3. Larva, Second Instar

The second-instar larva is modified eucoiliform (without thoracic appendages and caudal segment with a very short tail). This stage was observed between the 5th and 10th day after oviposition, when the host was in the pupa phase. It appears to last around 108 h. General aspects and measurements are given in Figures 3A–3C and Table 1. The body is more or less translucent, whitish or yellowish with a discernible gut (Fig. 3A) and wave-like segmentation on both ventral and dorsal sides and with some white globular fat particles; subcylindrical in shape, with a short and fleshy head; mouth with external oral papillae (Fig. 3C, see arrow); unidentate mandibles, with slightly sclerotized apices and slightly protuberant labial palpi; caudal segment with very short tail (Fig. 3B); anus opening dorsally, seen as an indentation in the contour of the posterior dorsal side (Fig. 3A).
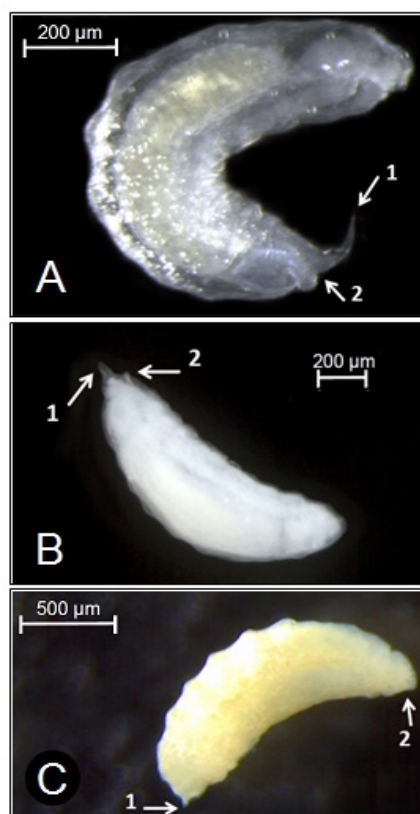

Figure 3. *Aganaspis daci* (Weld). Larval phase. Second instar: (**A–C**) body in lateral view showing the short tail [see arrow 1 in (**A–C**)], anus [see arrow 2 in (**A**)], oral papilla [see arrow 2 in (**C**)], and reminiscence of the ventral process [see arrow 2 in (**B**)].

3.2.4. Larva, Third Instar

The third-instar larva is hymenopteriform. This stage was found between the ninth and 14th day after oviposition. It appears to last around 100 h. General aspects and measurements are given in Figures 4A–4D and Table 1. The body is yellowish with white fat globules in the mesosoma and metasoma (Fig. 4A); subcylindrical in shape, with broad head (Figs. 4B, 4C). Spiracles (Figs. 4B, 4D) are apparent on the first metasomal segment; atrium with asperities. Dorso-laterally each segment bears one pair of tegumental differentiations (one sensorial structure on each side; Fig. 4C'). The anus terminal is in a central position as a transverse slit (Fig. 4A). Mouthparts with small and unidentate mandibles are apparent (Figs. 4B, 4D).
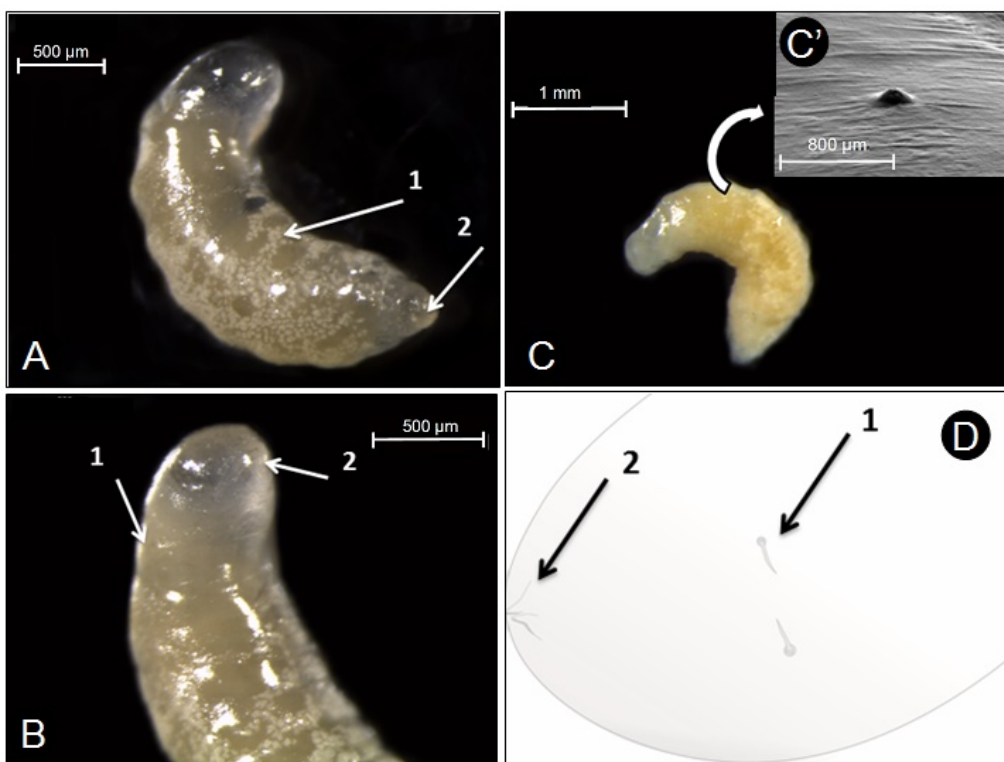

Figure 4. *Aganaspis daci* (Weld). Larval phase. Third instar: (**A, C**) body in lateral view showing the fat globules in mesosoma and metasoma (see arrow 1) and the anus (see arrow 2), and tegumental differentiations [(**C, C'**) shows a detail under SEM]. **B**: Anterior part of body in lateroventral view showing the spiracles [see arrow 1, detail in (**D**) where it is possible to see the asperities of the atrium] and mandibles [see arrow 2, detail in (**D**)].

3.2.5. Larva, Fourth Instar

The mature larva is like the previous instar hymenopteriform type. This stage was found between the 15th and 21st day after oviposition. It appears to live around 140 h. General aspects and measurements are shown in Figures 5A–5C and Table 1. The body is whitish with small white fat globules present in the metasoma and whose stomach content is easily discernible (Fig. 5B). The shape is subcylindrical with well-developed pleural lobes (Fig. 5C). The terminal anus is a transverse slit (Fig. 5C). In this instar, it is possible to observe the configuration of the cephalic sclerites on the head capsule (Fig. 5E), that show a marked difference with the previous instar, and several sensory structures (Fig. 5E). On both sides of the dorsolateral region of the prothorax there is a tiny seta (Fig. 5A). There are also several tegumental differentiations, most probably having a sensory function, that are either scattered (Fig. 5F) or arranged in rows or clusters on the tegument of the mesoma and metasoma. The spiracles (Fig. 5D) are present on all body segments, except the prothorax and last metasomal segment above the pleural lobes (Fig. 5 C) and walls of the atrium with asperities (Fig. 5A). The cranium (Figs. 5A–C, 5E) has two papilliform antennae with one apical sensillum (Fig. 5E). The epistoma and labrum are distinct, sclerotized, with sensory structures (Figs. 5E, 6C, 6C'). The labral sclerite is emarginated (Fig. 5E). The mandibles (Figs. 6A, 6B) have two sharp well sclerotized apical teeth. The maxillae and labium (Figs. 6A, 6C, 6D) have distinguishable sensory structures that could correspond to labial palpi, maxillary palpi and sensilla arranged behind labial palpi (Figs. 6C, 6D). A reduction was observed in the size of the predefecating mature larva to the prepupa (postdefecating mature larva; Fig. 6E), probably due to expulsion of the meconium.
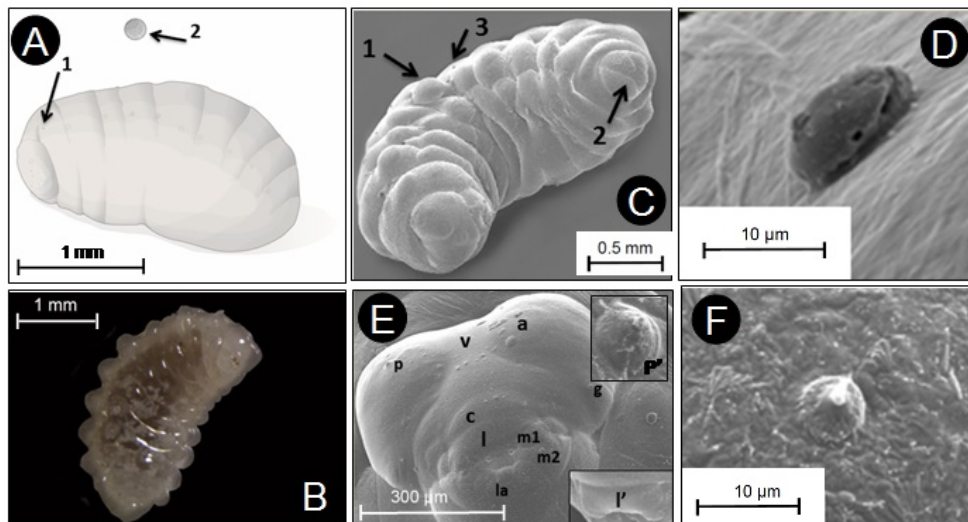
Figure 5. *Aganaspis daci* (Weld). Larval phase. Fourth instar: (**A–C**) body in lateral view showing the head and fat globules and stomach content (**B**), pleural lobes (see arrow 1), anus (see arrow 2), and location of the spiracles (see arrow 3) [(**C**) (under SEM); (**D**) (under SEM)] shows the prothoracic spiracle in detail, setae on the prothorax [see arrow 1, (**F**) showing a detail] and detailed view of the spiracles (atrium with asperities, see arrow 2) (**A**). **E**: (under SEM): cranium showing the vertex (v), antennal areas (a) with antennal papillae (p), cephalic sclerites [clypeus (c), labrum (l, l')] mouthparts (m1 = mandibles, m2 = maxilas; la = labium), sensory structures [e.g., gena setae (g)], and detail of antennal apical sensillum (p').
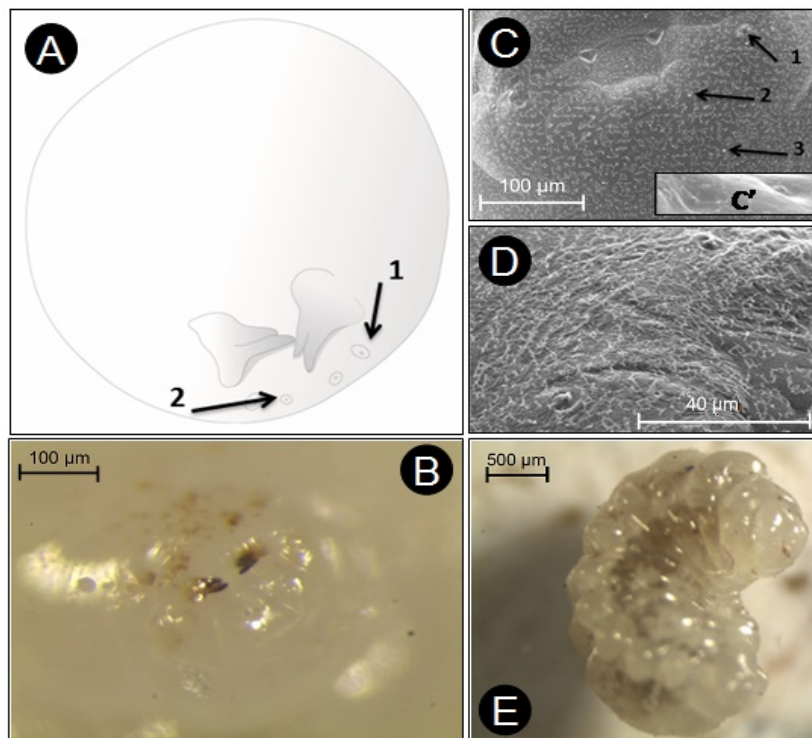

Figure 6. *Aganaspis daci* (Weld). Larval phase. Fourth instar: (**A, B**) mouthparts: mandibles, maxillary, and labial palpi [see arrow 1, 2 in (**A, C**)] and sensilla behind labial palpi [see arrow 3 in (**C**) and detail in (**D**)]. **C'**: Detail of the sensilla of the labrum. **E**: mature larva expulsing the meconium.

3.2.6. Pupa

General aspects are presented in Figures 7A, 7B, and Table 1. The body is naked, adecticous, and exarate. Initially, this immature stage is white but later pigmentation begins to appear until the dark adult coloring is reached. The most outstanding character of this phase lies in the presence of protuberances on the metasoma (Fig. 7B); by contrast, the corresponding area on the larval or adult metasoma is bare. The adults use their mandibles to chew a small irregular circular emergence hole (Figs. 7C, 7D) through the puparial wall. This instar lasts for 9 days. The males emerge in 4–7 days and the females in 7–9 days.
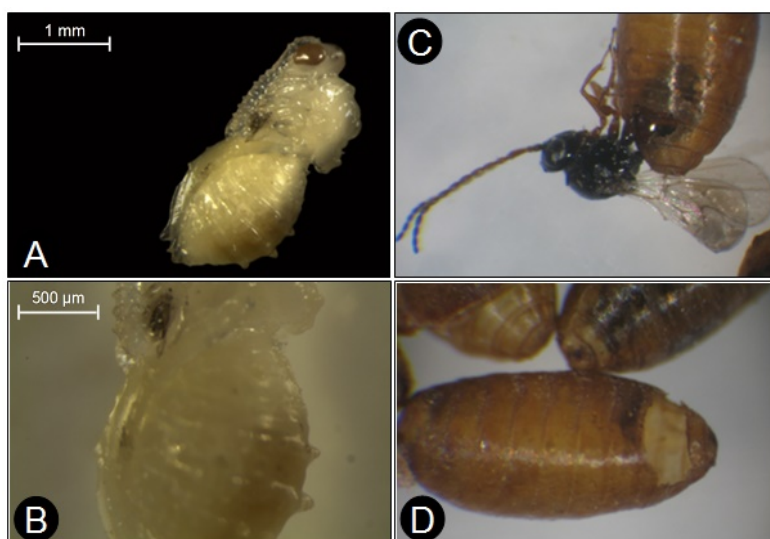

Figure 7. *Aganaspis daci* (Weld). Pupal and adult phase: Pupa: (**A, B**) body in lateral view, (**B**) shows the dorso-lateral metasomal protuberances in detail. Adult: (**C**) adult emerging from a *C. capitata* pupa. **D**: Puparium with an emergence hole.

3.3. Sensillar equipment on antennae and ovipositor

3.3.1. Antennae

In both species, female antennae are cylindrical and consist of 13 segments: a scape, a pedicel, and a flagellum consisting of 11 flagellomeres (Figs. 8A, 8D). In males of both species, 13 flagellomeres are present, so the antennae, also cylindrical, are composed of 15 segments (Figs. 9A, 9D). *A. pelleranoi* is larger than *A. daci*, and so has longer antennae (Table 2). Male/female ratio of antenna length is similar in both species (Table 2). Female antennae belong to the moniliform type (i.e., like a string of beads), while male antennae belong to the filiform type (i.e., linear and slender) (Figs. 8A, 8D, 9A, 9D). Neither female nor male antennae present a distally distinct club (i.e., a greatly enlarged apical flagellomer or flagellomeres of an antenna; Figs. 8B, 8E, 9B, 9E); however, in females, the apical segment (F11) is slightly longer than the next one (F10) (F11/F10 ratio similar in both species; Figs. 8A, 8D; Table 2); this does not

occur in males (Figs. 9A, 9D; Table 2). The flagellomeres in female moniliform antennae are distinctly separated by a narrow neck-like articulation, which is wider (i.e., placing segments further apart from one another) in *A. daci* than in *A. pelleranoi* (the width is similar but the antennae of *A. daci* are smaller) (Figs. 8A, 8D, 8C, 8F; Table 2). F1 in males of both species are swollen and excavated ventro-laterally. This modification, named "release and spread structure" (RSS; Isidoro et al., 1996), consists of a ridge and an excavation (Figs. 9C, 9F), both of which are perforated with pores (Fig. 10D). The length of RSS is similar in both species (Table 2), and covered most of F1, which is of similar length despite the overall inter-specific difference in antenna length (i.e., RSS is relatively longer in *A. daci*). Pores of RSS are similar in size in the two species, although they are much more visible in *A. daci* under SEM.

Sensilla found on the antennae protrude from the cuticle or sometimes lie within or beneath it. We recognized seven types of sensilla in both species: sensilla placoidea (SP), sensilla coeloconica type I (SCo-I), sensilla coeloconica type II (SCo-II), sensilla campaniformia (SCa), sensilla trichoidea type I (ST-I), sensilla trichoidea type II (ST-II) and sensilla trichoidea type III (ST-III). All types of sensilla were found in both sexes, except ST-II and ST-III, which were only found in males. The description of each sensilla type is given below.
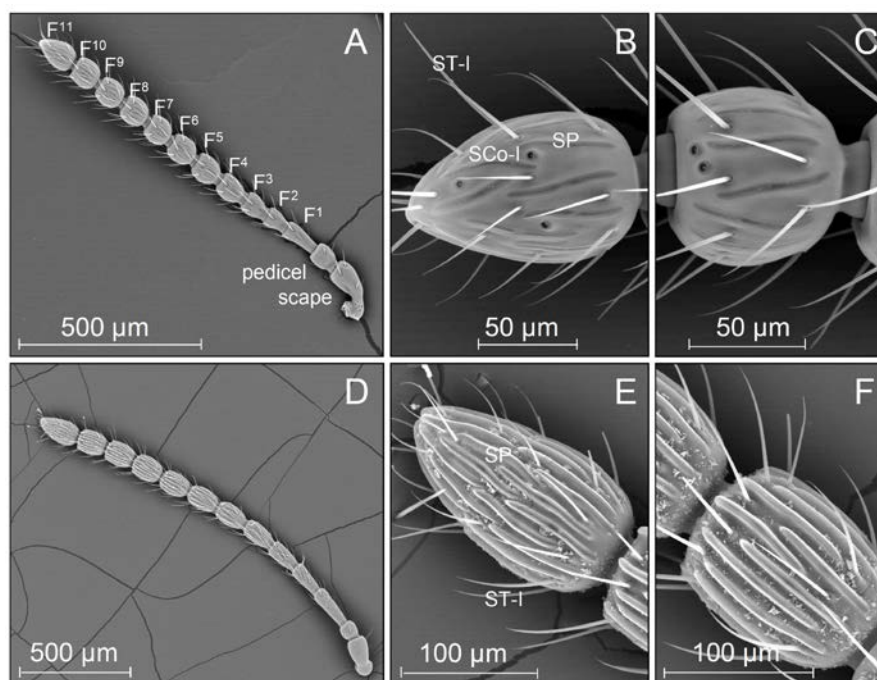
Figure 8. General aspect of the female antenna [(**A, D**) both in dorsal view] of *Aganaspis* spp., and of its F11 [(**B**) ventral view; (**E**) dorsal view] and F9 [(**C**) ventral view, (**F**) dorsal view]. **A–C**: *A. daci*; **D–F**: *A. pelleranoi*. SP, sensilla placoidea; SCo-I, sensilla coeloconica-type I; ST-I, sensilla trichoidea-type I.
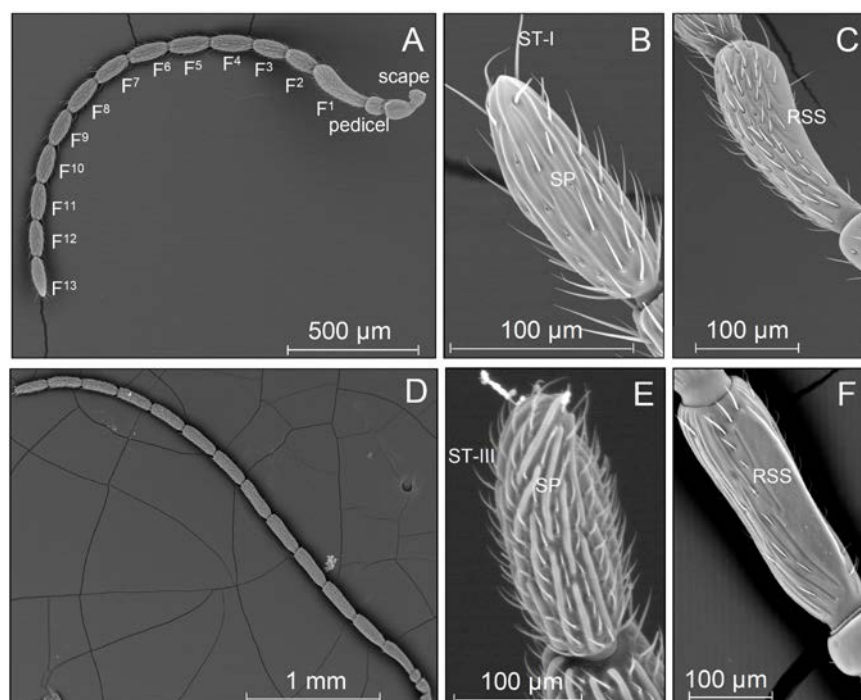

Figure 9. General aspect of the male antenna [(**A, D**) both in lateral view] of *Aganaspis* spp., and of its F13 [(**B**) lateral view; (**E**) dorsal view] and F1 [(**C**) lateral view; (**F**) ventral view]. **A–C**: *A. daci*; **D–F**: *A. pelleranoi*. SP, sensilla placoidea; ST-I, sensilla trichoidea-type I; ST-III, sensilla trichoidea-type III; RSS, release and spread structure.

Table 2. Measurements taken on the antennae and antennal sensilla of *Aganaspis daci* and *Aganaspis pelleranoi*. All measures are in μm.

| Variable	A. daci	A. pelleranoi
Antenna length	Females: 900–1000, males: 2000–2100	Females: 1800–2000, males: 3900–4000
Male/female ratio of antenna length	2	2
Length of apical segment (F11 for females and F13 for males)	Females: 110–114, males: 150–155	Females: 174–179, males: 258–270
Length of F10 (females) or F12 (males)	Females: 75–78, males: 140–150	Females: 120–129, males: 262–280
F11/F10 ratio (females)	1.5	1.5
F13/F12 ratio (males)	1	1
Width of the narrow neck-like articulation between flagellomeres of female antenna	15–18	15–18
Release and spread structure (RSS) in male antenna	220–240	220–240
Length of F1 in males	280–300	270–290
Area of RSS pores	1	1
SP length / flagellomer length	0.66–1	0.66–1
SP length	Females: 30–70, males: 70–90	Females: 60–100, males: 60–110
SP width	Females: 4–5, males: 4–6	Females: 6–8, males: 4–5
SCo-I peg diameter	1	1.5
SCo-II peg diameter	2	2
Diameter of the SCo-I "collared" pit from which the peg protrudes	3–4	3–4
SCa button-like nov diameter	0.5	0.5
ST-I length	Females: 50–60, males: 30–50	Females: 50–80, males: 30–50
ST-I width at the half length	2	2
ST-II length	20–50	20–50
ST-II width (at the half length)	1.5	1.5
ST-III length	15–30	15–30
ST-III width (at the half length)	2	2
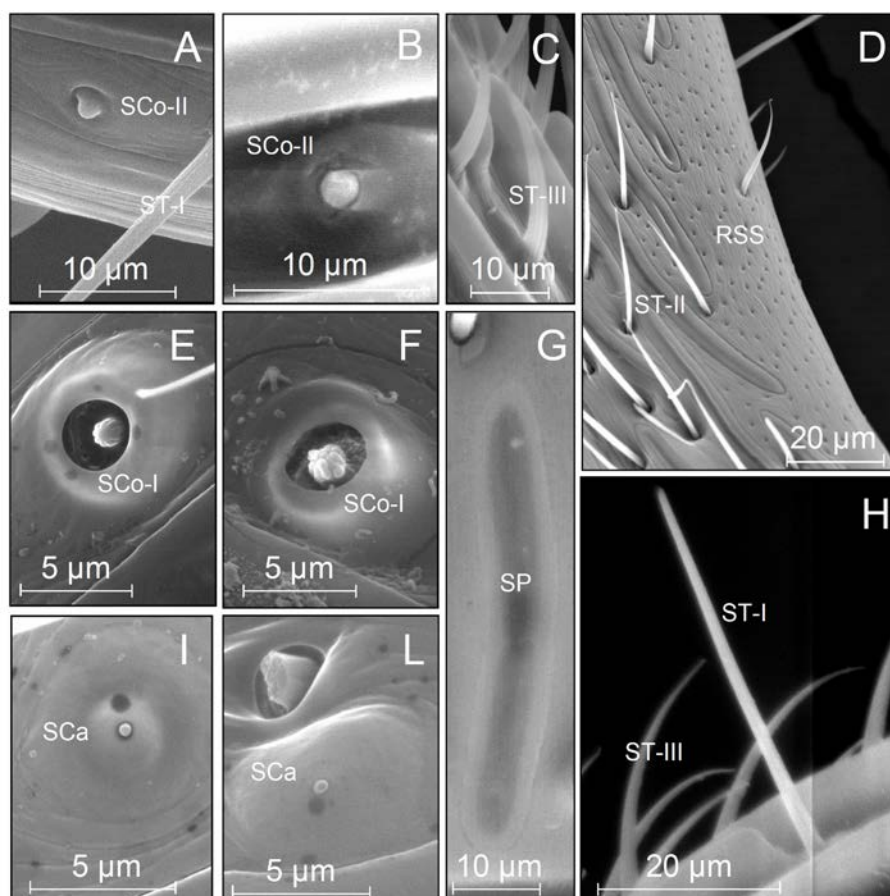
Figure 10. Different sensilla types found on the antennae of *Aganaspis* spp. **A, E, G, I**: *A. daci* female; (**F**) *A. pelleranoi* female; (**D, L**) *A. daci* male; (**B, C, H**) *A. pelleranoi* male. SP, sensilla placoidea; SCo-I, sensilla coeloconica-type I; SCo-II, sensilla coeloconica-type II; ST-I, sensilla trichoidea-type I; Sca, sensilla campaniformia; ST-I, sensilla trichoidea-type I; ST-II, sensilla trichoidea-type II; ST-III, sensilla trichoidea-type III; RSS, release and spread structure.

3.3.1.1. SP

The SP are the largest and the most conspicuous sensilla on the antennae of both sexes and species (Figs. 8B–8F, 9B–9F). They are multiporous, elongate, plate-like sensilla with a large surface area arising from the cuticle (*A. pelleranoi*) or almost lying flat against it (*A. daci*), and they are surrounded by a grooved gap (Figs. 8, 9, 10G). In both species, SP covers a large part of a flagellomer, and its length and width varies with species and sex, being overall larger in *A. pelleranoi* females (Figs. 8, 9; Table 2). SP occur on all flagellomeres both dorsally and ventrally, are aligned parallel to the antennal axis (Figs. 8, 9), and their number in each flagellomer (counted on dorsal side) is higher in *A. pelleranoi* (females: seven to nine, males: 20–30) than in *A. daci* (females: four to seven, males: seven to nine). In addition, in both sexes of *A. pelleranoi* SP is elevated more from a cuticular base of the flagellomer when compared to the flatter structure found in *A. daci*.

3.3.1.2. Sensilla Coeloconica

This type of poreless sensilla is of two distinct types. In the SCo-I the cuticular peg stands on the antennal surface and presents a "collar" of wrinkled cuticle surrounding the peg, which is set in a distinct cuticular depression (Figs. 10 E, 10F). Meanwhile in SCo-II, the peg is almost completely embedded within the antennal wall, communicating with the external environment only through a narrow opening (Figs. 10 A, 10B). The two types also differ in peg shape, this being very bulbous in SCo-I, with the stalk of the peg giving rise to finger-like projections joining at the tip (Fig. 10 E, 10F), and with a simpler, unsulked structure in SCo-II (Figs. 10A, 10B). Coeloconic sensilla are located ventrally, sometimes laterally, and are present in relatively low numbers in the antennae, and in particular SCo-II were found to be extremely rare, present only on F7–F11. On rare occasions, SCo-II were found in clusters of four to six on a single flagellomer. SCo-I were observed to have a more defined distribution on the antennal segments, being present in pairs or triplets (much more rarely in groups of four) from F2 to F11, generally distally, in both sexes and species. The shape of the SCo-I and SCo-II seems to differ between species: in particular in *A. daci* the peg of SCo-I is a bit smaller and the bulbous structure seems to be more organized and less "inflated" than in *A. pelleranoi* (Figs. 10A, 10B, 10E, 10F; Table 2).

3.3.1.3. SCa

SCa are characterized by a button-like knob with an irregular surface emerging from an opening in the center of a quite flattened, or slightly raised smooth circular cuticular disk (Figs. 10I, 10L; Table 2). They are located ventrally and are quite rare along the antenna, with just one sensillum per flagellomer (sometimes they were lacking), from F2 to F11 in both sexes and species, and often close to the SCo-I.

3.3.1.4. Sensilla Trichoidea

We found three different types of trichoid sensilla. All were observed to be long sensilla ending in a fine, sharp tip. They were abundant on all flagellomeres both ventrally and dorsally. ST-I was the only type we found in females, while all types were found in males. ST-I were the longest trichoid sensilla (Figs. 8, 9, 10A, 10H; Table 2), they can be either curved or not, and have longitudinal grooves. The longest and less curved ones were especially found laterally on the distal part of the flagellomeres, sometimes in a pair of two sensilla located at opposite positions along the segment width (Figs. 8, 9). ST-II are a bit shorter than ST-I, a bit more curved, thinner than ST-I, and they have less pronounced longitudinal grooves (Fig. 10D; Table 2). These sensilla are typically the only type found around the RSS on F1 (Fig. 10D). ST-III were the shortest trichoid sensilla, more curved than the other types, quite thick, and with deep

longitudinal grooves (Figs. 10C, 10H; Table 2). This sensilla type appeared to be much more abundant in *A. pelleranoi* than in *A. daci* (Figs. 9B, 9E).

3.3.2. Ovipositor

As in other hymenopteran parasitoids, the ovipositor of *Aganaspis* spp. consists of paired (Valva I) and unpaired valves (Valva II) (Fig. 11A). The paired valves articulate with the unpaired valve through a tongue-and-groove arrangement. In addition to the sensilla and some barbs present on the tip of the paired lower valves, a particular structure, the ovipositor clip (OC), is observed on the unpaired valve near the tip of the ovipositor at about 130–150 μm from the tip (Fig. 11D).

Sense organs were found on Valva I. These sensilla (OS) resemble coeloconic sensilla of type II (SCo-II) (Figs. 11B, 11C). The peg is about 1 μm in diameter and about 0.5 μm long. They are found distributed along the distal half of Valva I, having a characteristic arrangement with three pairs about 10 μm apart and with two sensilla in a pair at a distance of about 5 μm apart (Fig. 11B).
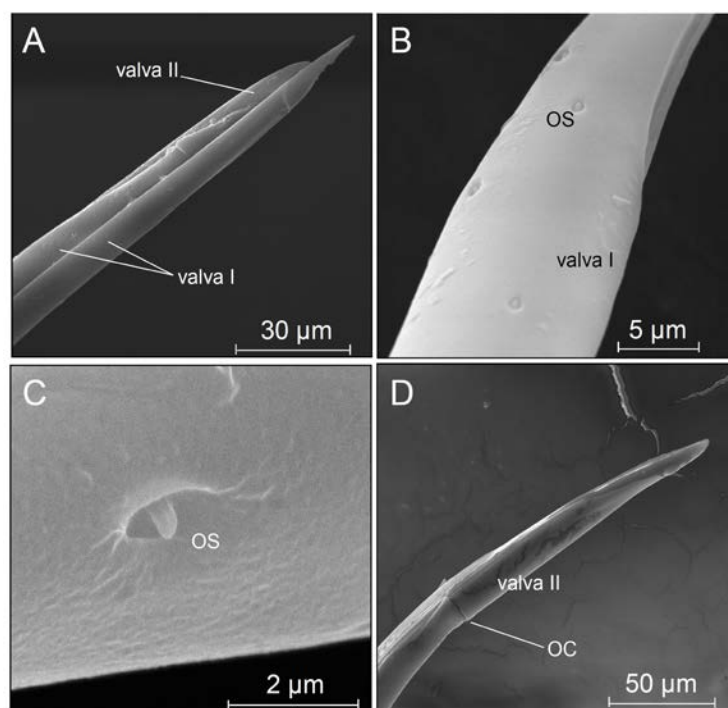

Figure 11. Ovipositor morpohological features and ovipositor sensilla in *Aganaspis* spp. (**A**) Distal part of the ovipositor of *A. daci*, showing the ventral paired Valva I and the dorsal fused Valva II; (**B**) closer view of a part of the Valva I of *A. daci* where the ovipositor sensilla (OS) are visible in pairs; (**C**) the coeloconic-like morphology of an OS in *A. daci*; (**D**) distal part of the ovipositor of *A. pelleranoi*, showing the ovipositor clip (OC) on the Valva II.

4. Discussion

4.1. Preimaginal stages

Data concerning the biology and development of *A. daci* under the indicated environmental conditions of temperature, photoperiod, and RH, using *C. capitata* as host, are similar to those obtained previously for this parasitoid on *Bactrocera dorsalis* (Hendel) (Diptera: Tephritidae) (Clausen et al., 1965). Nevertheless, the aforementioned author reported three larval instars in *A. daci*, while the present study proves the presence of four larval instars. Additionally, this study has established that the first instar larvae of *A. daci* have a pair of unidentate mandibles as indicated by Cals-Usciati et al. (1985), whereas Clausen et al. (1965) stated that the first instar larvae of this parasitoid do not possess visible mandibles.

A. daci presents a stalked egg, typical of the eucoline figitid. Like the egg of *A. pelleranoi* (Brèthes) (Ovruski, 1994), the egg of *A. daci* is covered by a thin chorion with a stalk at the anterior end and similarly, the stalk disappears when the parasitoid larva is completely formed and the egg is about to hatch. As in eggs of Hymenoptera parasitoids that are deposited internally, the chorion of *A. daci* eggs is smooth (Quicke, 1997; Tormos et al., 2007, 2009*a*, 2009*b*). As with cynipoid parasitoid eggs, the *A. daci* egg is divided into a relatively small and narrow egg body and a peduncule, which is not excessively thin or elongated. The eucoiliform early first-instar larva hatches from the membranes surrounding it via the strong muscular action of its tail, appendages, and body. It is also possible that the chorion is broken anteriorly by the mandibles, as reported by Ovruski (1994) in *A. pelleranoi*. In this respect, once the stalk has been lost in the *A. daci* egg, a specialized region is observed at the anterior end of the egg, where the egg shell is distinctly softer. This apparently specialized region of the egg shell, having the morphology of a micropylar region, corresponds more or less to the portion where the peduncle is located. Possibly, it facilitates the emergence of the young larva.

The morphology and development of the larval phase is similar to other figitids, although the following character states differentiate the larval instars of *A. daci* from most other larvae of known eucoilid parasitoids: (1) First-instar larva: (a) *A. daci*, like *A. pelleranoi*, lacks setae upon the mesosomal processes, differently from that reported by Clausen (1972) for *Trybliographa rapae* (Westwood); (b) *A. daci*, unlike *A. pelleranoi*, presents tegumental differentiations in the mesoma and first metasomal segment. (2) Immature (second and third instars) and mature larvae: in *A daci*, unlike *A. pelleranoi*, the third- and fourth- instar larvae present integument with tegumentary differentiations likely of sensory nature. The lack of detail provided by most descriptions of the eucoilid preimaginal phases does not allow for proper comparison to be made.

The mandibles of different larval instars of *A. daci* are described in less detail than other mouthpart structures because we were not able to obtain adequate SEM micrographs of them. Nevertheless, examining them under a stereomicroscope enabled us to characterize the immature larval instars (in this case unidentate) of the mature larva (in this case bidentate). Under a stereomicroscope, the structure of the first tooth, even the inner margin, was straight, smooth, unserrated, and similar to that reported for *A. pelleranoi* by Ovruski (1994).

With respect to development, the transition from endoparasitic to ectoparasitic life has also been reported for other eucoiline species (Ovruski, 1994; Melk & Govind, 1999). Regarding the time immature stages take to develop, differences observed with respect to other studies (e.g., Papadopoulos & Katsoyannos, 2003) are due to the fact that *A. daci* lays its eggs inside *C. capitata* larvae, which do not hatch until the host larva has formed a pupa. Furthermore, low temperatures, e.g., 20 ºC, slow development of the parasitized larvae, causing pupa formation of the different specimens to last longer. This implies an extended duration of the parasitoid immature stages.

4.2. Sensillar equipment

The present descriptions significantly enlarge our knowledge of antennal sensillar equipment in the Cynipoidea, given that previous detailed information is available for only a couple of species (*T. rapae, Dryocosmus kuriphilus*; Yasumatsu) (Butterfield & Anderson, 1994; Romani et al., 2010*b*).

The sensilla placodea of *Aganaspis* spp. are similar to those found in the few other cynipids studied to date (Butterfield & Anderson, 1994; Romani et al., 2010*b*), and thus probably have the same olfactory function described in other Hymenoptera (Akers & Getz, 1992; Ochieng et al., 2000). The greater abundance of SP found in males compared to females is a common feature in parasitoid Hymenoptera (Baaren et al., 1999; Ochieng et al., 2000; Bleeker et al., 2004), perhaps because males have to recognize more stimuli than females (e.g., plant volatiles and sex pheromones; Whitman & Eller, 1992; Alborn et al., 1995). Possibly, for a similar reason, males also possess two types of sensilla (ST-II and ST-III) which are not present in females.

The SCo-I have been detected in many species of parasitic Hymenoptera (e.g., Bleeker et al., 2004; Onagbola & Fadamiro, 2008), including Cynipoidea (Butterfield & Anderson, 1994; Romani et al., 2010*b*). SCo-II have previously been described in braconid wasps (Ochieng et al., 2000; Bleeker et al., 2004) but, as far as we know, never in Cynipoidea. The function of SC is still not clear, being described as either olfactory organs (Keil, 1999) or thermo or hygro receptors (Altner et al., 1983).

SCa with similar morphology to that found in *Aganaspis* spp. were observed in both parasitic and aculeate Hymenoptera (sometimes under the name of sensilla coelocapitula; e.g. Romani et al., 2010*b*; Meng et al., 2012; Polidori et al., 2012). However, here we provide the first evidence that SCa are also present in Cynipoidea. Amputation experiments suggested that their function is not olfactory (Dietz & Humphreys, 1971); instead, electrophysiological studies suggest that SCa are thermo hygroreceptors (Lacher 1964; Merivee et al., 2003).

With the present data is difficult to assess the function of the commonest trichoid sensilla (ST-I) in *Aganaspis* spp. The long ST-I were hypothesized to be chemo receptors by contact and the short ST-I to be mechanoreceptors in previously studied cynipoids (Butterfield & Anderson, 1994; Romani et al., 2010*b*). This is the first description of ST-II and ST-III in Cynipoidea, and their function remains unknown.

The OS found on *Aganaspis* spp. are similar to those described for other Figitidae (Gutiérrez, 1970; Brown & Anderson, 1998; Lenteren et al., 2007). Such coeloconic sensilla were suggested to be mechanoreceptors (Altner & Prillinger, 1980; Brown & Anderson, 1998). Because the pegs protrude above the surface of the cuticle, these sensilla may be used to detect external stimuli during ovipositor movement through the substrate. Other few types of sensilla found on the ovipositor of Figitidae (Brown & Anderson, 1998; Lenteren et al., 2007) were not detected in *Aganaspis* spp.

5. Conclusions

This study has added a considerable amount of new detailed morphological data on both immature stages and adults in a group of parasitic wasps. Past studies were mostly lacking in the fine level of analysis achieved only through combined SEM and light microscopy. Finer detailed morphological studies of such wasps, which are parasitoids of important fruit pests, are necessary because successful biological control against pests depends, among other things, on the ability to recognize natural parasitoid species even at larval stages. However, this is only possible by (microscopic) comparison with previously acquired morphological data on the different phases of development. Furthermore, microscopic analysis is extremely useful to test for numerous effects, such as different nutritional regimes or different temperatures on the size and morphology of both larval and adult parasitoids. Such information is useful to optimize rearing conditions, before releasing the wasps in the field to control pests. It is also important to understand the sensory basis of host recognition, and one important step in this respect is to analyze the morphology of sensory structures in detail, and to eventually compare them among wasp species differing in host niche spectrum and host specialization. From this point of view, further investigations by means of histological techniques and SEM observations are necessary to better understand the function of each type of sensilla.

Acknowledgments

References

AKERS, R.P. & GETZ, W.M. (1992). A test of identified response classes among olfactory receptor neurons in the honey-bee worker. *Chem Senses* **17**, 191−209.

ALBORN, H.T., LEWIS, W.J. & TUMLINSON, J.H. (1995). Host-specific recognition kairomone for the parasitoid *Microplitis croceipes* (Cresson). *J Chem Ecol* **21**, 1697−1708.

ALTNER, H. (1977). Insect sensillum specifity and structures: An approach to a new typology. In *Olfaction and Taste VI*, Le Magnen, L. & MacLeod, P. (Eds.), pp. 295−303. Paris: IRL.

ALTNER, H. & PRILLINGER, L. (1980). Ultrastructure of invertebrate chemo-, thermo-, and hygroreceptors and its functional significance. *Int Rev Cytol* **67**, 69−139.

ALTNER, I., HATT, H. & ALTNER, H**.** (1983). Structural properties of bimodal chemo- and mechanoreceptive setae on the pereiopods chelae of the crayfish, *Austropotamobius torrentium*. *Cell Tissue Res* **228**, 357−374.

ANDLEEB, S., SHAHID, M.S. & MEHMOOD, R. (2010). Biology of parasitoid *Aganaspis daci* (Weld) (Hymenoptera: Eucoilidae). *Pak J Sci Ind Res* **53**, 201−204.

BAAREN, J. VAN, BOIVIN, G., BOURDAIS, D. & ROUX, O. (2007). Antennal sensilla of hymenopteran parasitic wasps: Variations linked to host exploitation behavior. In *Microscopy: Science, Technology, Applications and Education*, Méndez-Vilas, A. & Díaz, J. (Eds.), pp. 345−352. Badajoz, Spain: Formatex.

BAAREN, J. VAN, BOIVIN, G., LE LANNIC, J. & NÉNON, J.P. (1999). Comparison of antennal sensilla of *Anaphes victus* and *A. listronoti* (Hymenoptera: Mymaridae), egg-parasitoids of Curculionidae. *Zoomorphology* **119**, 1−8.

BARANOWSKI, R., GLENN, H. & SIVINSKI, J. (1993). Biological control of the Caribbean fruit fly (Diptera: Tephritidae). *Fla Entomol* **76**, 245–251.

BEITIA, F., PÉREZ-HINAREJOS, M., SANTIAGO, S., GARZÓN, E., TARAZONA, I. & FALCÓ, J.V. (2009). Control biológico con parasitoides. *Levante agricola* **385**, 145–150.

BELLOWS, T.S. & VAN DRIESCHE, R.G. (1999). Life table construction and analysis for evaluating biological control agents. In *Handbook of Biological Control. Principles and Applications of Biological Control*, Bellows, T.S. & Fisher, T.W. (Eds.), pp. 199–223. San Diego, CA: Academic Press.

BLEEKER, M.A.K., SMID, H.M., AELST, A.C., VAN LOON, J.J.A. & VET, L.E.M. (2004). Antennal sensillae of two parasitoid wasps: A comparative scanning electron microscopy study. *Microsc Res Tech* **63**, 266–273.

BROWN, P.E. & ANDERSON, M. (1998). Morphology and ultrastructure of sense organs on the ovipositor of *Trybliographa rapae*, a parasitoid of the cabbage root fly. *J Insect Physiol* **44**, 1017–1024.

BUTTERFIELD, A. & ANDERSON, M. (1994). Morphology and ultrastructure of antennal sensilla of the parasitoid, *Trybliographa rapae* (Westw.) (Hymenoptera: Cynipidae). *Int J Insect Morphol Embryol* **23**, 11–20.

CALLAHAN, P.S. (1975). Insect antennae with special reference to the mechanism of scent detection and the evolution of the sensilla. *Int J Insect Morphol Embryol* **4**, 381–430.

CALS-USCIATI, J., CALS, P. & PRALAVORIO, R. (1985). Functional adaptations of the feeding mechanism in the primary larva of *Trybliographa daci* Weld (Hymenoptera, Cynipoidea), endoparasitoid of the Mediterranean fruit fly *Ceratitis capitata*. *C R Seances Acad Sci, Ser 3* **300**, 103–108.

CLAUSEN, C.P. (1972). *Entomophagous Insects*. New York: Hafner Publishing Company.

CLAUSEN, C.P. (1978). *Introduced Parasites and Predators of Arthropod Pests and Weeds: A World Review*. Washington D.C.: U.S. Department of Agricultural Handbook.

CLAUSEN, C.P., CLANCY, D.W. & CHOCK, Q.C. (1965). Biological control of the oriental fruit fly (*Dacus dorsalis* Hendel) and other fruit flies in Hawaii. *Agri Res Serv* **1322**, 1–102.

DÍAZ, N.B., GUIMARAES, J.A. & GALLARDO, F.E. (2006). Systematic review of species of the genus *Aganaspis* Lin (Hymenoptera: Figitidae: Eucoilinae). *T Am Entomol Soc* **132**, 271−277.

DIETZ, A. & HUMPHREYS, J. (1971). Scanning electron microscopic studies of antennal receptors of the worker honey bee, including *Sensilla campaniformia. Ann Entomol Soc Am* **64**, 919–925.

EL-HENEIDY, A.H. & RAMADAN, M.M. (2010). *Bactrocera zonata* (Saunders) status and its natural enemies in Egypt. In *8th International Symposium on Fruit Flies of Economic Importance*, p. 115. Valencia, Spain: Editorial Universitat Politècnica de València.

EVANS, H.E. (1987). Cynipoidea. In *Immature Insects*, Stehr, F.W. (Ed.), pp. 665−667. Dubuque, IA: Kendall/Hunt Publishing Co.

GUIMARAES, J.A. & ZUCCHI, R.A. (2004). Parasitism behavior of three species of Eucoilinae (Hymenoptera: Cynipoidea: Figitidae) fruit fly parasitoids (Diptera) in Brazil. *Neotrop Entomol* **33**, 217−224.

GUTIÉRREZ, A.P. (1970). Studies on host selection and host specificity of the aphid hyperparasite *Charips victrix* (Hymenoptera: Cynipidae). 6. Description of sensory structures and a synopsis of host selection and host specificity. *Ann Entomol Soc Am* **63**, 1705−1709.

ISIDORO, N., BIN, F., COLAZZA, S. & VINSON, S.D. (1996). Morphology of antennal gustatory sensilla and glands in some parasitoids Hymenoptera with hypothesis on their role in sex and host recognition. *J Hym Res* **5**, 206−239.

JERVIS, M.A., COPLAND, M.J.W. & HARVEY, J.A. (2005). The life cicle. In *Insects as Natural Enemies. A Practical Perspective*, Jervis, M.A. (Ed.), pp. 112−196. Amsterdam: Kluwer Academic Publishers.

KEIL, T.A. (1999). Morphology and development of the peripheral olfactory organs. In *Insect Olfaction*, Hansson, B.S. (Ed.), pp. 5−47. New York: Springer-Verlag.

LACHER, V. (1964). Elektrophysiologische Untersuchungen an einzelnen Rezeptoren für Geruch, Kohlendioxid, Luftfeuchtigkeit and Temperatur auf den Antennen der Arbeitsbiene und der Drohne (Apis mellifera L). *Z Verg Physiol* **48**, 587−625.

LENTEREN, J.C. VAN, RUSCHIONI, S., ROMANI, R., VAN LOON, J.J.A., QIU, Y.T., SMID, H.M., ISIDORO, N. & BIN, F. (2007). Structure and electrophysiological responses of gustatory organs on the ovipositor of the parasitoid *Leptopilina heterotoma*. *Arthropod Struct Dev* **36**, 271–276.

LLÁCER, E., URBANEJA, A., GARRIDO, A. & JACAS, J. (2005). Morphology and development of immature stages of *Galleosomyia fausta* (Hymenoptera: Eulophidae: Tetrastichinae). *Ann Entomol Soc Am* **98**, 747–753.

MELK, J.P. & GOVIND, S. (1999). Developmental analysis of *Ganaspis xanthopoda*, a larval parasitoid of *Drosophila melanogaster*. *J Exp Biol* **202**, 1885–1896.

MENG, Z.J., YAN, S.C., YANG, C.P. & RUAN, C.C. (2012). Asymmetrical distribution of antennal sensilla in the female *Anastatus japonicus* Ashmead (Hymenoptera: Eupelmidae). *Microsc Res Tech* **75**, 1066–1075.

MERIVEE, E., VANATOA, A., LUIK, A., RAHI, M., SAMMELSELG, V. & PLOOMI, A. (2003). Electrophysiological identification of cold receptors on the antennae of the ground beetle *Pterostichus aethiops*. *Physiol Entomol* **28**, 88–96.

NIEVES-ALDREY, J.L., VÅRDAL, H. & RONQUIST, F. (2004). Comparative morphology of terminal-instar larvae of Cynipoidea: Phylogenetic implications. *Zool Scr* **34**, 15–36.

OCHIENG, S.A., PARK, K.C., ZHU, J.W. & BAKER, T.C. (2000). Functional morphology of antennal chemoreceptors of the parasitoid *Microplitis croceipes* (Hymenoptera: Braconidae). *Arthropod Struct Dev* **29**, 231–240.

ONAGBOLA, E.O. & FADAMIRO, H.Y. (2007). Morphology and development of *Pteromalus cerealellae* (Ashmead) (Hymenoptera: Pteromalidae) on *Callosobruchus maculatus* (F.) (Coleoptera: Chrysomelidae). *Biocontrol* **53**, 737–750.

ONAGBOLA, E.O. & FADAMIRO, H.Y. (2008). Scanning electron microscopy studies of antennal sensilla of *Pteromalus cerealellae* (Hymenoptera: Pteromalidae). *Micron* **39**, 526–535.

OVRUSKI, S.M. (1994). Immature stages of *Aganaspis pelleranoi* (Brethes) (Hymenoptera: Cynipoidea: Eucoilidae), a parasitoid of *Ceratitis capitata* (Wied.) and *Anastrepha* spp. (Diptera: Tephritidae). *J Hym Res* **3**, 233–239.

OVRUSKI, S.M. & ALUJA, M. (2002). Mating behavior of *Aganaspis pelleranoi* (Brèthes) (Hymenoptera: Figitidae, Eucoilinae), a fruit fly (Diptera: Tephritidae) larval parasitoid. *J Insect Behav* **15**, 139–151.

OVRUSKI, S.M., ALUJA, M., SIVINSKI, J. & WHARTON, R. (2000). Hymenopteran parasitoids on fruit-infesting Tephritidae (Diptera) in Latin American and the southern United States: Diversity, distribution, taxonomic status and their use in fruit fly biological control. *Integrated Pest Manag Rev* **5**, 81–107.

PAPADOPOULOS, N.T. & KATSOYANNOS, B.I. (2003). Field parasitism of *C. capitata* larvae by *Aganaspis daci* in Chios, Greece. *Biocontrol* **48**, 191–195.

POLIDORI, C., JORGE GARCÍA, A. & NIEVES-ALDREY, J.L. (2012). Antennal sensillar equipment in closely related predatory wasp species (Hymenoptera: Philanthinae) hunting for different prey types. *C R Biol* **335**, 279–291.

QUICKE, D.L.J. (1997). *Parasitic Wasps*. London: Chapman & Hall.

ROMANI, R., ISIDORO, N. & BIN, F. (2010*a*). Antennal structures used in communication by egg parasitoids. In *Egg Parasitoids in Agroecosystems with Emphasis on Trichogramma*, Consoli, F.L., Parra, J.R.P. & Zucchi, R.A. (Eds.), pp. 57–96. New York: Springer.

ROMANI, R., RONDONI, G., GRAGNOLI, L., PERGOLARI, P., SANTINELLI, C., ROSSI STACCONI, M.V. & RICCI, C. (2010*b*). Indagini bio-etologiche e morfologiche su *Dryocosmus kuriphilus* Yasumatsu. In *Atti Accademia Nazionale Italiana di Entomologia Anno LVIII*, 97–104.

ROSKAM, J.C. (1982). Larval characters of some eurytomid species Hymenoptera, Chalcidoidea. *Proc Kon Ned Akad Wet* **85**, 293–305.

TORMOS, J., ASÍS, J.D., GAYUBO, S.F. & MARTÍN, M.A. (2004). Descriptions of the final instar of *Eurytoma nodularis* and *E. heriadi* (Hymenoptera: Eurytomidae). *Fla Entomol* **87**, 278–282.

TORMOS, J., BEITIA, F., BÖCKMANN, E.A. & ASÍS. J.D. (2009*a*). The preimaginal stages and development of *Spalangia cameroni* Perkins (Hymenoptera: Pteromalidae) on *Ceratitis capitata* (Wiedemann) (Diptera: Tephritidae). *Micron* **40**, 646–658.

TORMOS, J., BEITIA, F., BÖCKMANN, E.A., ASÍS, J.D. & FERNÁNDEZ, S. (2009*b*). The preimaginal phases and development of *Pachycrepoideus vindemmiae* (Hymenoptera, Pteromalidae) on Mediterranean fruit fly, *Ceratitis capitata* (Diptera, Tephritidae). *Microsc Microanal* **15**, 422–434.

TORMOS, J., FRAGO, E., SELFA, J., ASÍS, J.D., PUJADE-VILLAR, J. & GUARA, M. (2007). Description of the final instar larva of *Trichomalopsis peregrina* (Hymenoptera, Pteromalidae), with data and comments on the preimaginal stages. *Fla Entomol* **90**, 180–183.

TORMOS, J., PARDO, X., JIMÉNEZ, R., ASÍS, J.D. & GAYUBO, S.F. (2003). Descriptions of adults, immature stages and venom apparatus of two new species of Dacnusini: *Chorebus pseudoasphodeli* sp. n., parasitic on *Phytomyza chaerophili* Kaltenbach and *C. pseudoasramenes* sp. n., parasitic on *Cerodontha phragmitophila* Hering (Hymenoptera: Braconidae: Alysiinae; Diptera: Agromyzidae). *Eur J Entomol* **100**, 393–400.

VÅRDAL, H., SAHLEN, G. & RONQUIST, F. (2003). Morphology and evolution of the cynipoid egg (Hymenoptera). *Zool J Linn Soc* **139**, 247–260.

WELD, L.H. (1951). A new species of Trybliographa (Hymenoptera: Cynipidae). *Proc Hawaii Entomol Soc* **14**, 331–332.

WHARTON, R.A., GILSTRAP, F.E., RHODEI, R.H., FISCHEL, M.M. & HART, W.G. (1981). Hymenopterous egg-pupal and larval-pupal parasitoids of *Ceratitis capitata* and *Anastrepha spp.* (Diptera: Tephritidae) in Costa Rica. *Entomophaga* **26**, 285–290.

WHITMAN, D.W. & ELLER, F.J. (1992). Orientation of *Microplitis croceipes* (Hymenoptera: Braconidae) to green leaf volatiles: Dose-response curves. *J Chem Ecol* **18**, 1743–1753.